Scaling solutions and finite-size effects in the Lifshitz–Slyozov theory

Dieter W. Heermann and Li Yixue*

Institut für theoretische Physik
Universität Heidelberg
Philosophenweg 19
D-69120 Heidelberg
and
Interdisziplinäres Zentrum
für Wissenschaftliches Rechnen
der Universität Heidelberg

Kurt Binder

Institut für Physik, Universität Mainz
Staudinger Weg 7
D-55099 Mainz

February 16, 1996

Abstract

We have developed a finite-size scaling theory for the late stages of growth following a quench. This theory predicts how the distribution of droplets depends on the finite extension of a system as it appears for example in computer simulations. From the scaling properties of the distribution we obtain scaling laws for the average droplet size. To check the developed theory we have performed Monte Carlo simulations of the three-dimensional Ising model using several system sizes. Strong finite-size effects occur already when the average linear dimension of the largest cluster is only about one sixth of the lattice size.

*Permanent address: Department of Physics, Xinjiang University, P.R. China

1 Introduction

Two component mixtures show a rich morphology in non-equilibrium [1]. A typical situation is shown in Figure 1 where the system is brought into the non-equilibrium state by a quench from an initial equilibrium state. The theory for the following evolution in terms of the morphology of the system, if the volume fraction of the minority phase is small, was founded by Lifshitz, Slyozov and Wagner [2, 3]. The theory considered how the typical domains or droplets of the minority phase evolve in time. Initially there is a metastable state, i.e., a supersaturated matrix from which small droplets are nucleated decreasing the supersaturation and eventually nucleation stops. Once this nucleation stage of the phase separation process has ended, the further approach to equilibrium proceeds via the coarsening of the droplets. The theory predicts a power law behaviour for the average droplet size. The theory was later modified by incorporating also the coagulation of droplets [4] and also considering the effects of non-vanishing concentration of the minority phase [5]. It was also observed in experiments [6] and computer simulations [7] that the evolution also shows a scaling, for example for the structure factor. Such a scaling behaviour leads to the idea that there must also be a scaling with respect to the finiteness of the system. Such a scaling can be developed for critical phenomena [8], as well as for first-order phase transitions [9]. In this paper we want to apply the ideas of the finite-size scaling theory to the problem of the growth of droplets. This question is pertinent to computer simulations as well as experiments. In computer simulations the systems are by necessity always small and in experiments grain boundaries may lead to small sample sizes. Also there is a growing interest in phase separation in thin film geometry [10] and porous materials [11]. For the latter case, effects of a finite pore radius R_0 have been considered [11]. We shall present a critical comparison with the latter work below.

2 The Scaling Theory

In this section, we only focus on a very simple-minded approach related to the limiting case, where the volume fraction of the growing droplets of the minority phase is very small. As is well known [5], at finite volume fraction the *screening length* of the diffusion field needs to be considered as a second characteristic length in addition to the typical droplet size. Finite size scaling with two characteristic lengths is rather complicated [8] and should be considered as a second step in a later work on the present problem, but it is discarded in the present paper giving a first step only.

In the thermodynamic limit, the *Lifshitz–Slyozov* theory [2] can be obtained from the solution of the differential equation

$$\frac{\partial}{\partial t}\bar{n}_\ell(t) \,+\, \frac{\partial}{\partial \ell}\left\{\bar{n}_\ell(t) R' \ell^{1-2/d}[\Delta h(t) \,-\, f_o(1-1/d)\,\ell^{-1/d}]\right\} \,=\, 0 \qquad (1)$$

{cf. Eqs. (3.39) and (3.42) of [4]} together with the condition of mass conservation {cf. Eq.(3.44)} of [4]}

$$\frac{d}{dt}\int_0^\infty d\ell\,\ell\,\bar{n}_\ell\,(t) \,=\, 0 \quad . \qquad (2)$$

In these equations, $\bar{n}_\ell(t)$ denotes the average number of clusters with volume ℓ at time t; d is the dimensionality; R' is the prefactor of a kinetic rate, f_o the prefactor of a surface free energy (both volume dependences of the rate and the surface free energy assume compact clusters). Finally, $\Delta h(t)$ is the time–dependent chemical potential difference [$\Delta h(\infty) = 0$ when upon completion of phase separation macroscopic domains coexist]. Here $\Delta h(t)$ follows from the constraint that Eq.(2) is obeyed at every instant of time.

In a finite system, we expect that $\Delta h(t)$ will approach a nonzero limit $\Delta h(\infty)$; also, clusters cannot become arbitrarily large, but are rather than that unable to exceed some maximum volume $\tilde{L}$ (which follows from the condition that the total volume of B–atoms is distributed according to the lever rule): if the total volume of the system is denoted as V and we work at a concentration c_B in between the concentrations $c_{coex}^{(1)}$, $c_{coex}^{(2)}$ at the coexistence curve, we must require

$$V c_B \, = \, \tilde{L} c_{coex}^{(2)} \, + \, (V - \tilde{L}) c_{coex}^{(1)} \, = \, V c_{coex}^{(1)} \, + \, \tilde{L} \Delta c \quad ,$$

where Δc is the concentration difference between coexisting phases. Hence

$$[c_B - c_{coex}^{(1)}] V \, = \, \tilde{L} \Delta c \; , \quad \tilde{L} = \frac{c_B - c_{coex}^{(1)}}{\Delta c} \, V \quad . \tag{3}$$

Then the distribution function $\bar{n}_\ell^{(\tilde{L})}(t)$ will depend also on the variable $\tilde{L}$. In addition, this maximum volume $\tilde{L}$ appears as an upper limit of integration in the condition of mass conservation, and Eq.(2) is thus replaced by

$$\frac{d}{dt} \int_0^{\tilde{L}} d\ell \bar{n}_\ell^{(\tilde{L})}(t) = 0 \quad . \tag{4}$$

In the following, we shall assume that $\bar{n}_\ell^{(\tilde{L})}(t)$ still satisfies the differential equation, Eq.(1), but of course also $\Delta h(t)$ has to be replaced by the function $\Delta h^{(\tilde{L})}(t)$, which follows from Eq.(4) and now exhibits an $\tilde{L}$–dependence.

We note that already our starting point (Eqs.1 - 4) differs fundamentally from the treatment of size effects by Slyozov, Schmelzer and Möller [11], where it was assumed that there is no effect of the finite radius R_0 of pores on the droplet size distribution apart from preventing droplets to grow a radius $R > R_0$, which in our notation would mean droplet volumes $l > V$. From Eq.(3) it is obvious that a strong size effect must appear for $l \leq \tilde{L}$. Since what we seek are scaling solutions of Eqs.(1), (4), we first indicate the solution of Eqs.(1), (2) in the limit of $V \to \infty$ in terms of a scaling treatment. One starts from the ansatz {cf. Eq.(3.43) of [4]

$$\bar{n}_\ell(t) = t^y \, \widetilde{n} \, (\ell t^{-x}) \quad , \tag{5}$$

where $\widetilde{n} \, (z)$ is the scaling function (of argument $z \equiv \ell t^{-x}$), and the exponents x, y must be chosen such that Eq.(5) actually solves Eqs.(1), (2). From Eq.(2) one immediately finds

$$\frac{d}{dt} \, t^{y+2x} \int_0^\infty z \, dz \, \widetilde{n} \, (z) \, = \, 0 \quad \Longrightarrow y \, = \, -2x \quad . \tag{6}$$

Next we indicate how Eq.(2) leads via Eq.(1) to a determination of the chemical potential difference, and what Eq.(5) has to do with its time dependence. We start by rewriting Eq.(2) as

$$0 = \frac{d}{dt}\int_0^\infty \bar{n}_\ell(t)\ell d\ell$$
$$= \int_0^\infty \frac{\partial \bar{n}_\ell(t)}{\partial t}\,\ell d\ell \;=\; -\int_0^\infty \frac{\partial}{\partial \ell}\Big\{\bar{n}_\ell(t)R'\ell^{1-2/d}[\Delta h(t) - f_o\Big(1-\frac{1}{d}\Big)\,\ell^{-1/d}]\Big\}\,\ell d\ell\,,$$

where Eq.(1) has been used. Now we proceed by integrating by parts to find

$$0 = \int_0^\infty d\ell\Big\{\bar{n}_\ell(t)R'\ell^{1-2/d}[\Delta h(t) - f_o(1-\frac{1}{d})\ell^{-1/d}]\Big\} \quad .$$

This is the desired equation, and it already yields $\Delta h(t)$, namely

$$\Delta h(t) = f_o\Big(1-\frac{1}{d}\Big)\;\frac{\int_0^\infty d\ell \bar{n}_\ell(t)\ell^{1-3/d}}{\int_0^\infty d\ell \bar{n}_\ell(t)\ell^{1-2/d}} \quad . \tag{7}$$

Now, inserting the scaling assumption, Eq.(5) yields a simple power law behaviour for $\Delta h(t)$,

$$\Delta h(t) = \; f_o(1-\frac{1}{d})\,c_1 t^{-x/d}\;, \quad c_1 \equiv \frac{\int_0^\infty dz\;\widetilde{n}\;(z)z^{1-3/d}}{\int_0^\infty dz\;\widetilde{n}\;(z)z^{1-2/d}} \quad . \tag{8}$$

We now insert both Eqs.(5), (8) into Eq.(1), using ($z = \ell t^{-x}$) and eliminating all powers of ℓ by the corresponding powers of z , we obtain

$$\frac{1}{f_o(1-\frac{1}{d})R'}\Big\{-2x\;\widetilde{n}\;-xz\frac{\partial\;\widetilde{n}}{\partial z}\Big\} = \frac{\partial}{\partial z}\Big\{t^{2x+1}(t^{-3x-x/d}\,z^{1-2/d}\,t^{x-2x/d})\;\widetilde{n}\;(z)[z^{-1/d}-c_1]\Big\}$$
$$t^{2x+1}(t^{-3x-x/d}\,z^{1-2/d}\,t^{x-2x/d}) = t^{1-3x/d}\,z^{1-2/d} \quad . \tag{9a}$$

Obviously, the scaling ansatz Eq.(5) can solve Eq.(1) only if the extra power of t found in the above equation cancels, which happens for

$$x = d/3 \quad . \tag{9b}$$

The solution of the remaining differential equation for $\widetilde{n}\;(z)$ is presented in [4]; for $d = 3$ it reproduces the results of *Lifshitz and Slyozov* [2]. From Eqs.(9), (5) we immediately obtain the familiar result for the average cluster volume,

$$\bar{\ell}(t) \equiv \int_0^\infty d\ell\ell^2\,\bar{n}_\ell(t)\,\Big/\int_0^\infty d\ell\ell\bar{n}_\ell(t) = t^x\int_0^\infty dz z^2\;\widetilde{n}\;(z)\,\Big/\int_0^\infty dz z\;\widetilde{n}\;(z) \propto t^{d/3}\;. \tag{10}$$

Now we turn to the modifications of this treatment {when the finite size of the system must be taken into account, Eq.(2) is being replaced by Eq.(4)}. First we point

out that an explicit result for the time dependence of $\Delta h(t)$ as expressed by $\bar{n}_\ell(t)$ can still be found, by a treatment analogous to that which led to Eq.(7). We perform exactly the same steps as above, but with Eq.(4) instead of Eq.(2),

$$0 = \frac{d}{dt}\int_0^{\tilde{L}} \bar{n}_\ell(t)\ell d\ell = \int_0^{\tilde{L}} \frac{\partial \bar{n}_\ell(t)}{\partial t}\ell d\ell = -\int_0^{\tilde{L}} \frac{\partial}{\partial \ell}\{...\}\,\ell d\ell \quad .$$

Care has to be exerted in the integration by parts, since the upper integration limit now contributes,

$$\int_0^{\tilde{L}} v'ud\ell = uv\Big|_0^{\tilde{L}} - \int_0^{\tilde{L}} u'vd\ell \;=\; u(\tilde{L})\,v(\tilde{L}) \;-\; \int_0^{\tilde{L}} u'vd\ell \quad .$$

Thus

$$\begin{aligned}
0 &= -\tilde{L}\Big\{\bar{n}_{\tilde{L}}(t)R'\tilde{L}^{1-2/d}\Big[\Delta h(t) - f_o\Big(1-\frac{1}{d}\Big)\tilde{L}^{-1/d}\Big]\Big\} \\
&\quad + \int_0^{\tilde{L}} d\ell\Big\{\bar{n}_\ell(t)R'\ell^{1-2/d}\Big[\Delta h(t) - f_o\Big(1-\frac{1}{d}\Big)\ell^{-1/d}\Big]\Big\}\,, \\
\Delta h(t)\Big[&-\tilde{L}\bar{n}_{\tilde{L}}(t)\,R'\tilde{L}^{1-2/d} + \int_0^{\tilde{L}} R'\,\bar{n}_\ell\,(t)\,\ell^{1-2/d}d\ell\Big] \\
&= \Big[-\tilde{L}\bar{n}_{\tilde{L}}(t)\,R'\tilde{L}^{1-3/d}f_o(1-\frac{1}{d}) + \int_0^{\tilde{L}} R'd\ell\bar{n}_\ell(t)\ell^{(1-3/d)}\,f_o\Big(1-\frac{1}{d}\Big)\Big]
\end{aligned}$$

Hence Eq.(7) is replaced by

$$\Delta h(t) = f_o\Big(1-\frac{1}{d}\Big)\,\frac{\int_0^{\tilde{L}} d\ell\ell^{1-3/d}\,\bar{n}_\ell(t) - \tilde{L}\bar{n}_{\tilde{L}}(t)\tilde{L}^{1-3/d}}{\int_0^{\tilde{L}} d\ell\ell^{1-2/d}\,\bar{n}_\ell(t) - \tilde{L}\bar{n}_{\tilde{L}}(t)\tilde{L}^{1-2/d}} \quad . \tag{11}$$

The final equilibrium is described by a single cluster at size $\tilde{L}$, so then, no other clusters being present, the contribution from the integrals can be omitted in Eq.(11), hence obtaining an explicit result for $\Delta h(\infty)$:

$$\Delta h(\infty) = f_o\Big(1-\frac{1}{d}\Big)\tilde{L}^{-1/d} \quad . \tag{12}$$

Of course, Eq.(12) is consistent with direct thermodynamic analyses of that situation [12]. Eq.(12) can be found more simply from Eq.(1) requiring that $\lim_{t\to\infty}\{\frac{\partial}{\partial t}\bar{n}_\ell(t)\} = 0$, which is obtained if the square bracket in Eq.(1) vanishes.

We now generalize the scaling assumption, Eq.(5), requiring that $\bar{n}_\ell^{(\tilde{L})}(t)$ depends on two scaled combinations only, rather than depending on three variables l, $\tilde{L}$, t separately:

$$\bar{n}_\ell^{(\tilde{L})}(t) \;=\; t^{-2x}\;\widetilde{n}\;(\ell t^{-x},\,\ell/\tilde{L}) \;=\; t^{-2x}\;\widetilde{n}\;\Big(z,\frac{z}{\tilde{L}t^{-x}}\Big) \quad . \tag{13}$$

If Eq.(13) holds, it is easy to find the scaling structure which replaces the simple power law for $\bar{\ell}(t)$, Eq.(10):

$$\bar{\ell}(t) \;=\; \int_0^{\tilde{L}} d\ell \ell^2 \bar{n}_\ell^{(\tilde{L})}(t)/const \;=\; t^x \int_0^{\tilde{L}t^{-x}} \frac{dz z^2}{const}\; \widetilde{n}\left(\frac{z}{\tilde{L}t^{-x}}\right) \equiv\; t^x f(\tilde{L}t^{-x}) \quad , \qquad (14)$$

where now $f(\tilde{L}t^{-x})$ is the appropriate scaling function. To evaluate it explicitly, we would have to solve the equations which determine $\widetilde{n}\,(z,z')$. In the following we shall not attempt to do this explicitly; we shall only show that Eq.(13) is indeed consistent with Eqs.(1), (4) and that x is still given as $x = d/3$ {Eq.(10)}. First we show that the power law, Eq.(8), is replaced by a scaling analogous to Eq.(14), if Eq.(13) is inserted into Eq.(11),

$$\Delta h(t)$$
$$= \; f_o(1-\frac{1}{d})t^{-x/d}\, \frac{\int_0^{\tilde{L}t^{-x}}\; dz z^{1-3/d}\; \widetilde{n}\;(z, \frac{z}{\tilde{L}t^{-x}}) - \tilde{L}t^{-x}\; \widetilde{n}\;(\tilde{L}t^{-x},1)(\tilde{L}t^{-x})^{1-3/d}}{\int_0^{\tilde{L}t^{-x}} dz z^{1-2/d}\; \widetilde{n}\;(z, \frac{z}{\tilde{L}t^{-x}}) - \tilde{L}t^{-x}\; \widetilde{n}\;(\tilde{L}t^{-x},1)(\tilde{L}t^{-x})^{1-2/d}} \qquad (15a)$$

which has the structure of

$$\Delta h(t) \;=\; f_o(1-1/d)t^{-x/d}\; \widetilde{h}\;(\tilde{L}t^{-x}) \quad . \qquad (15b)$$

Comparison of Eq.(15b) with Eq.(12) fixes the asymptotic behaviour of the scaling function $\widetilde{h}\;(z)$ defined by Eq.(15),

$$\widetilde{h}\;(z) \;\longrightarrow\; z^{-1/d}\;, \quad for\;\; z \to 0 \qquad (16)$$

just as we may conclude from Eq.(14) that

$$f(z) \;\longrightarrow\; z\;, \quad for\;\; z \to 0 \quad , \qquad (17)$$

in order that $\bar{\ell}(\infty) = \tilde{L}$.

While Eqs.(1), (5), (8) combined to yield an ordinary differential equation, Eq.(9a), from Eqs.(1), (13), (15) we find a partial integro–differential equation for $\widetilde{n}\;(z,z')$:

$$\frac{1}{f_o(1-\frac{1}{d})R'}\Big\{ -2x\; \widetilde{n}\;(z, \frac{z}{\tilde{L}t^{-x}}) \;-\; xz\, \frac{\partial\; \widetilde{n}}{\partial z}\,(z,z'\,\big|_{z'=z/\tilde{L}t^{-x}}\Big\}$$
$$= \frac{\partial}{\partial z}\Big\{ z^{1-2/d}\; \widetilde{n}\;(z, \frac{z}{\tilde{L}t^{-x}})[z^{-1/d} - \widetilde{h}\;(z)]\Big\} \qquad , \qquad (18)$$

where $\widetilde{h}\;(z)$ in turn depends on $\widetilde{n}\;(z,z')$ via Eq.(15), and Eq.(9b) was involved again to eliminate extra t–factors. While Eq.(2) together with Eq.(5) only helped to fix the exponent y {see Eq.(6)}, in our case it yields the additional equation from Eqs.(4) and (13):

$$(\tilde{L}t^{-x})^3\; \widetilde{n}\;(\tilde{L}t^{-x},1) \;=\; \int_0^{\tilde{L}t^{-x}} dz z^2\, \frac{\partial\; \widetilde{n}\;(z,z')}{\partial z'}\,\Big|_{z'\,=\,z/\tilde{L}t^{-x}} \quad . \qquad (19)$$

Unfortunately, an explicit solution of Eqs.(15), (18), (19) has not been found. Thus we can only infer qualitative conclusions. From Eq.(14) we find with $f(z) = z f_1(z)$ that $\bar{\ell}(t) = \tilde{L} f_1(\tilde{L} t^{-x})$, where $f_1(0) = 1$ [because of Eq.(17)], and $f_1(z \gg 1) \to 1/z$, in order to recover Eq.(10) in that limit. Qualitatively we hence expect a behaviour where (c.f. Figures 2,3) $df_1(z)/dz$ has a maximum at a value z_{max} of order unity. Since the definition of z implies for the corresponding time

$$\tilde{L} t_{max}^{-x} = z_{max}\,, \; t_{max} = (\tilde{L}/z_{max})^{1/x} \quad ,$$

we find $t_{max} \propto \tilde{L}^{3/d}$ for the corresponding time.

It is also interesting to ask where the maximum rate of growth occurs. We define a rate $\bar{R}(t)$ of cluster growth as

$$\bar{R}(t) = \frac{d\bar{\ell}}{dt} \quad . \tag{20}$$

For this discussion it is convenient to redefine $f_1(z) = f_2(z'')$ where $z'' = 1/z$. Then

$$\bar{R}(t) = \tilde{L}(df_2/dz'')xt^{x-1}/\tilde{L} = xt^{x-1}\, df_2/dz'' \quad .$$

The maximum of $\bar{R}(t)$ for $d = 3$, where $x = 1$, simply corresponds to the maximum of df_2/dz''. Now we know that $f_2(\infty) = 1$ and $f_2(z'' \to 0) \longrightarrow z''$. There are two possibilities to interpolate between these two limits:
(a) f_2 has its maximum slope at $z'' = 0$. This possibility would imply that the scaling region essentially starts after the inflection point of $\bar{\ell}(t)\, vs.\, t$ curves has been reached. This implies $t_{max} \approx const$ (independent of $\tilde{L}$) or $t_{max} \propto \tilde{L}^Y$ with $Y < 1/x$.
(b) $f_2(z'')$ has its maximum slope at $z''_{max} > 0$. Then we would predict that the inflection point of $\bar{\ell}(t)$ vs. t curves must scale as

$$t_{max} = (\tilde{L}/z''_{max})^{1/x} \propto \tilde{L} \quad (for\ d = 3) \quad . \tag{21}$$

Clearly, case (a) involves the simplest possibility, a monotonic decrease of df_2/dz'' with z''; and moreover, it seems to be consistent with simulations.

3 Simulation Results

The above developed finite-size scaling theory for the late stages of growth makes prediction for the droplet distribution and the average domain size. To check these we have carried out Monte Carlo simulations [13, 14, 15] of the three-dimensional Ising model. The concentration was fixed during the runs to $c_B = 0.048$. This concentration is well inside the two-phase region for the temperatures of $T/T_c = 0.59$ and 0.5. On the other hand, both parameters were adjusted such that we are not too far into the two-phase region where the classical concepts of the metastable state [16, 17, 18] are invalid [19, 20, 21]. At these low temperatures far below T_c, it is approrpiate to define clusters simply in terms of neighbouring groups of occupied sitesin the lattice gas model.

Because of the conserved concentration we used the Kawasaki-exchange algorithm [22]. The lattice linear sizes which we simulated were $L = 40, 50, 60, 80, 96$. In Table 3 we have summarized the data on the number of quenches over which we have averaged.

In Figures 4 and 5 we show the development of the cluster size of the largest cluster in the system following a quench and the development of the average cluster size. The average cluster size is a measure for the typical cluster size and is defined in the numerical calculation by the average over the average cluster size of the quenches

$$< l_i > (t) = \sum_{l}^{l_{max_i}} l^2 (n_l)_i(t) / \sum_{l}^{l_{max_i}} l(n_l)_i(t) \tag{22}$$

$$< l > (t) = \frac{1}{n} \sum_{i}^{n} < l_i > (t) \tag{23}$$

where n is the number of quenches. This implies that we performed for this quantity no binning for the distribution.

Of course, the development of the largest cluster is not a continuous event. The largest cluster at time t_0 may not be the same as the one at $t_0 + 1$. The largest cluster at time t_0 may have split into fragments or two clusters may have coalesced. The density which we have used is quite low so that clusters on average are far apart. We nevertheless have observed coalescence and fragmentation events.

The most interesting feature of Figures 4,5 is the clear evidence that very strong finite-size effects are already present when the average size of the largest cluster, the linear dimension $< l_{max} >^{1/3}$, is a factor six smaller than the linear dimension L of the system. E.g., at $t \approx 8000$MCS a value $< l_{max} > \approx 600$ corresponds to about $< l_{max} >^{1/3} \approx 8$ but even at $L = 50$ there is still a strong finite-size effect. This confirms our preliminary observation [23] and shows that one has to carefully watch out for finite-size effects in simulation studies of phase separation, at least for off-critical situations. Note that this cluster volume is about one order of magnitude smaller than the cluster volume $\tilde{L}$ describing the final equilibrium ($\tilde{L} \approx c_B L^3 = 6000$ for $L = 50$).

The evolution of the average cluster size shows three distinct time windows for the temperature $T/T_c = 0.59$. There is an initial increase in the average cluster size followed by an even stronger increase and then a levelling off. The initial increase is due to the finite lifetime of the metastable state. The system needs some time to overcome the nucleation barrier, which is small but larger than kT. In the later stages we can clearly

L	$T/T_c = 0.5$	$T/T_c = 0.59$
30	100	100
40	100	100
50	50	112
60	50	50
70	50	22
80	-	10
96	-	10

see the effect of the finiteness of the mass in the system. The growth of the average droplet size terminates. This levelling off is also seen in the growth of the largest cluster.

The lower temperature of $T/T_c = 0.5$ does not show an initial metastable state. The growth starts immediately following the quench. Because of the absence of a metastable state we will see later also a slight difference in the scaling behaviour.

Note that the apparent plateau seen in Figs. 4-6 for $L = 30$ does not mean that for this size the final equilibrium state with only one droplet of size $\tilde{L} \approx c_B L^3 = 12.96$ has been reached: We see that $< l_{max} >$ is still less than $\tilde{L}/2$ and that $< l > \ll < l_{max} >$, i.e. there are still many smaller droplets present.

Figure 6 shows the distribution of droplet sizes at three different times during the evolution. These times correspond to the three time windows. To obtain the distributions we used a binning for the larger sizes. The smaller sizes (less than $s = 100$) were not binned. The figure shows the redistribution of material from the smaller sizes to the larger sizes. For comparison we have shown in Figure 6 the evolution of the distribution for a smaller system size.

The flatness of the distribution at $l \approx 20 - 200$ for times $t \geq 10000$ in Figure 6 means that in the mass distribution ln_l there will develop a pronounced minimum near the size $l^* \approx 20$. Clusters with $l < l^*$ represent 'homophase fluctuations' of the weakly supersaturated background matrix [4], only the large droplets ($l > l^*$) are modelled by the Lifshitz-Slyozov theory there as described in Section II.

The scaling of the average domain size is shown in Figure 7. The smallest lattice shows no scaling behaviour for the higher temperature. The larger lattices show for later times a scaling. The scaling curve appears as an envelope of the scaled average cluster sizes for both temperatures. For the lower temperature the scaling starts for times immediately following the quench, whilst it departs soon from the scaling curve.

Following equation (13) we can now check the finite-size scaling of the characteristic droplet concentration n_{l^*}. The result is shown in Figure 8. We obtain a reasonable scaling behaviour considering the still large scatter in the distributions. As is obvious from Eq. (13), the full droplet size distribution $\tilde{n}_l^{(\tilde{L})}(t)$ in finite geometry even in the finite size scaling limit still depends on two arguments, namely the scaling varibales lt^{-x} and $l\tilde{L}$. Thus the scaled distribution is not a single curve but a family of curves. Since our data are effected both b statistical errors and corrections to scaling, any such plot of the full distribution is confusing and not presented here.

Comparing the predicted scaling function f_1 (c.f. eq (19) and Figure 2 we note that our system sizes are still too small to reach into the $1/z$ behaviour where we would find the asymptotic growth law (c.f. eq (10). We are also still one order of magnitude away from the saturation value of f_1 at $z = 0$. This means that we are in the neighbourhood of z_{max}.

4 Discussion and Conclusion

The aim of this paper is to draw attention to finite-size effects on the coarsening behaviour of droplets. Such finite-size effects occur in computer experiments - which usually apply $L \times L \times L$ geometry and periodic boundary conditions - and in real systems where a constrained geometry often is considered (phase separation in porous

media [11], thin film geometry [10], etc.). In this latter case, one must consider the combination of finite-size and surface effects, and this is clearly beyond the scope of the present paper, since we feel one should understand the finite-size effects first before one goes on to such a more intricate problem.

Even for the case of *pure* finite-size effects we consider a simplifying limit. We consider the case where the volume fraction ϕ of the minority phase (contained in the growing droplets) is negligibly small. In this case, for the linear dimension $L \to \infty$ the simple Lifshitz-Slyozov theory [2] holds, and one need not deal with the complicated problems of the *screening* of the diffusion field, whose gradients drive coarsening. It has been suggested that these screening effects lead to intermediate power laws of a distinct character [5], and in addition characteristic lengths (such as the *screening length*) come into play. The screening length develops with time in a manner different from the droplet linear dimension [5]. These phenomena may lead to strong deviations from a simple finite size scaling picture.

Our phenomenological theory of the finite-size effects is tested by Monte Carlo simulations and fair agreement is found. Unfortunately, it is not possible to make the volume fraction ϕ of the minority phase as small as would be desirable in view of the above remarks. For small volume fraction, there is an extended regime of time where initially a metastable state exists, and one has to wait until sufficiently many nucleation events have occurred. Only after nucleation has essentially stopped does one enter the regime of validity of the Lifshitz-Slyozov theory. For very small volume fraction ($\phi \leq 10^{-2}$) one thus needs extremely long simulation runs to enter this regime, and huge lattice sizes are also needed since the number of growing precritical droplets needs to be large in any case. Even with present computing facilities this regime of $\phi \leq 10^{-2}$ is not yet accessible. Both our simulation results and our phenomenological description (Sec. II) disagree with a recent theory [11] on coarsening in porous materials. The latter predicts a finite-size effect only via the growth of a delta-function peak in the droplet size distribution at the maximum allowed droplet size ($\tilde{L}$ in our case). However, we find pronounced effects already for $l_{max} \ll \tilde{L}$.

In conclusion, we hope that the present work will motivate other workers studying coarsening phenomena with simulations to carefully watch out for size effects. Experimental studies of coarsening in pores or thin films of controlled geometry would be most interesting.

References

[1] For recent reviews see: K. Binder, in Phase Transformations in Materials, ed. P. Haasen, Materials Science and Technology, Vol. 5 VCH Verlag, Weinheim, 1991 and S. Komura and H. Furukawa, eds. Dynamics of Ordering Processes in Condensed Matter, Plenum Press, New York, 1991

[2] I. M. Lifshitz and V. V. Slyozov, *J. Phys. Chem. Solids* 19, 35 (1961)

[3] W. Wagner *Z. Elektro Chem.* **65** 581 (1961)

[4] K. Binder, *Phys. Rev. B* **15**, 4425 (1977)

[5] M. Tokuyama and Y. Enomoto *Phys. Rev. E* **47**, 1156 (1993), and references therein

[6] Y.C. Chou and W.I. Goldburg, *Phys. Rev. A* 23 858 (1981), for reviews see Ref.1 and G. Kostorz, preprint, and T. Hashimoto, in Materials Science and Technology, Vol. 12, Structure and Properties of Polymers, ed. E.L. Thomas, VCH Verlag, Weinheim, 1993

[7] J. Marro, J.L. Lebowitz, and M.H. Kalos, *Phys. Rev. Lett* **43** 282 (1979) and more recent work is reviewed in Ref.1

[8] For recent reviews, see V. Privman (ed.) Finite Size Scaling and the numerical Simulation of Statistical Systems, World Scientific, Singapore, 1990, and K. Binder, in Computational Methods in Field Theory, eds. H. Gausterer and C.B. Lang, Springer Heidelberg, 1992

[9] K. Binder, K. Vollmayr, H.P. Deutsch, J.D. Reger, and M. Scheucher, *Int. J. Mod. Phys. C* **3** 253, (1992)

[10] S. Puri and K. Binder, *J. Stat. Phys* **77**, 145 (1994), and references therein.

[11] V.V. Slyozov, J. Schmelzer and B. Möller, *J. Crystal. Growth* **132**, 419 (1993); F. Aliev, W.I. Goldburg, and X.L. Wu, Phys. Rev. E **47**, R3834 (1993), and references therein

[12] H. Furukawa and K. Binder, *Phys. Rev.* A26, 556 (1982)

[13] M.H. Kalos and P.A. Whitlock, *Monte Carlo Methods*, Vol. 1, Wiley, New York, 1986

[14] D.W. Heermann, *Computer Simulation Methods in Theoretical Physics* 2nd ed., Springer Verlag, Heidelberg, 1990

[15] K. Binder and D.W. Heermann, *Monte Carlo Simulation in Statistical Physics: An Introduction*, Springer Verlag, Heidelberg, 1988

[16] R. Becker and W. Döring, *Ann. Phys. (Leipzig)*, **24**, 719 (1935)

[17] J.W. Cahn and J. Hilliard, *J. Chem. Phys.*, **31**, 688 (1959)

[18] J.S. Langer, *Annals of Phys.* **41**, 108 (1967)

[19] K. Binder, *Phys. Rev. A*, **29**, 341 (1984), and in Ref.1

[20] D.W. Heermann and W. Klein, *Phys. Rev. Lett.* **50**, 1962 (1983)

[21] W. Klein, *Phys. Rev. Lett.* **47**, 1569 (1981)

[22] K. Kawasaki, in *Phase Transitions and Critical Phenomena*, Vol. 2, C. Domb and M.S. Green, eds. Academic Press, London (1972)

[23] K. Binder and D.W. Heermann, in Scaling Phenomena in Disordered Systems, eds. R. Pynn and A. Skjeltrop, Plenum Press, New York (1985)

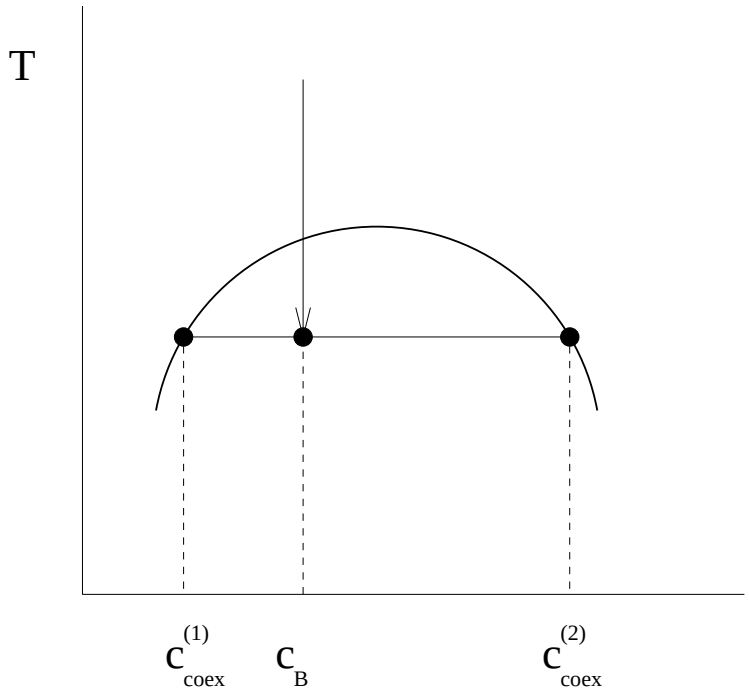

Figure 1: Generic phase diagram with a quench indicated. The equilibrium values for the two phases are also indicated.

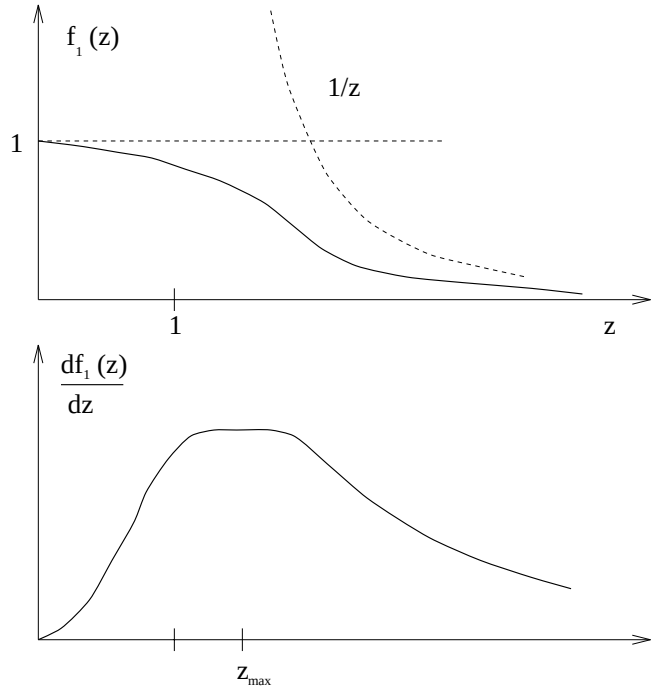

Figure 2: The function f_1 is a redefinition of the scaling function dreived in this paper. It is the scaling function as used in the plots of the simulation results. Shown is the qualitative behaviour of the function itself and its derivative which corresponds to the growth rate of the droplets

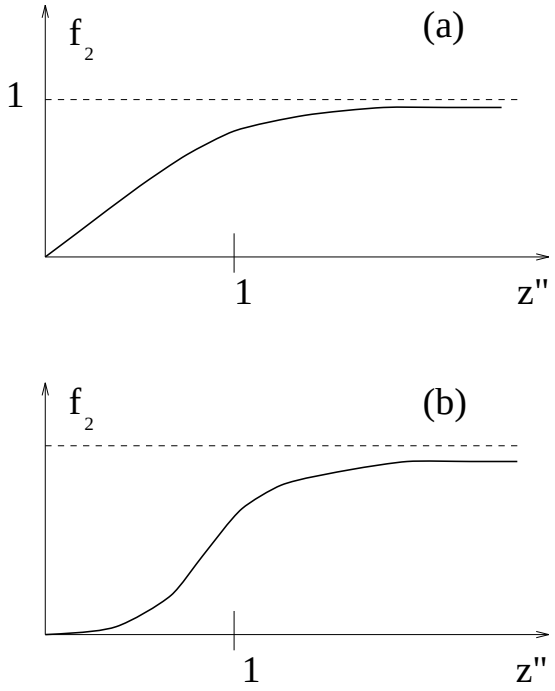

Figure 3: Qualitative behaviour of the function f_2 derived from the scaling function. (a) and (b) show the possible interpolations between the two limiting cases $z'' = 0$ and $z'' = \infty$

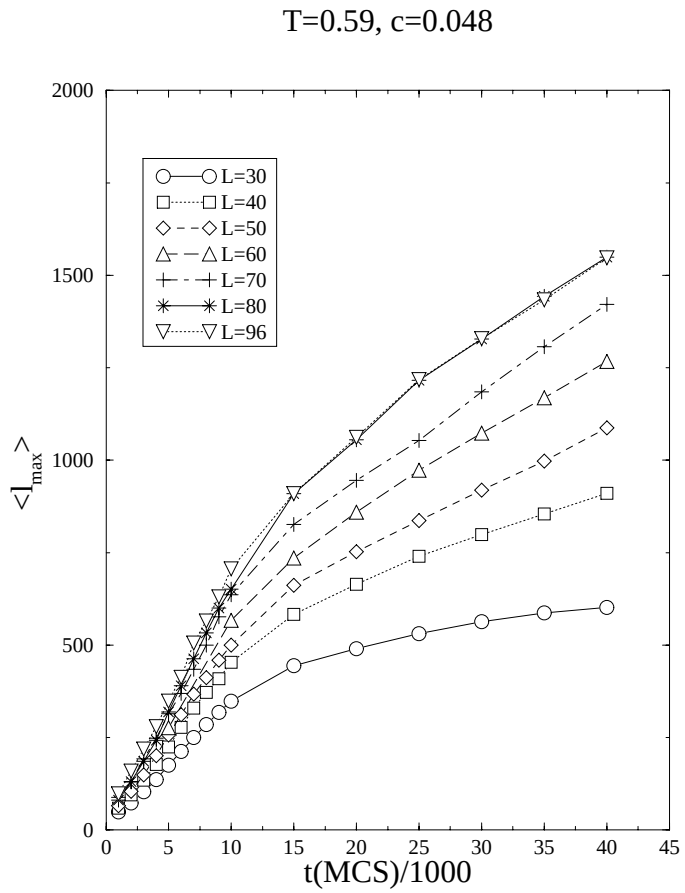

Figure 4: Time and size dependence of the number of atoms in the largest cluster found after a quench

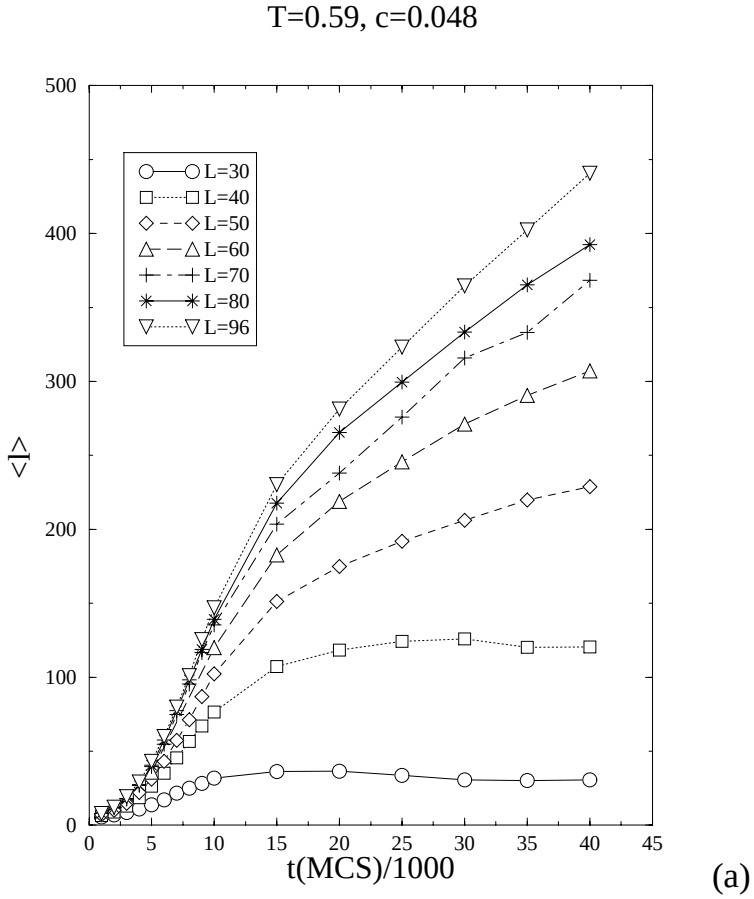

Figure 5: Time and size dependence of the average droplet size after a quench

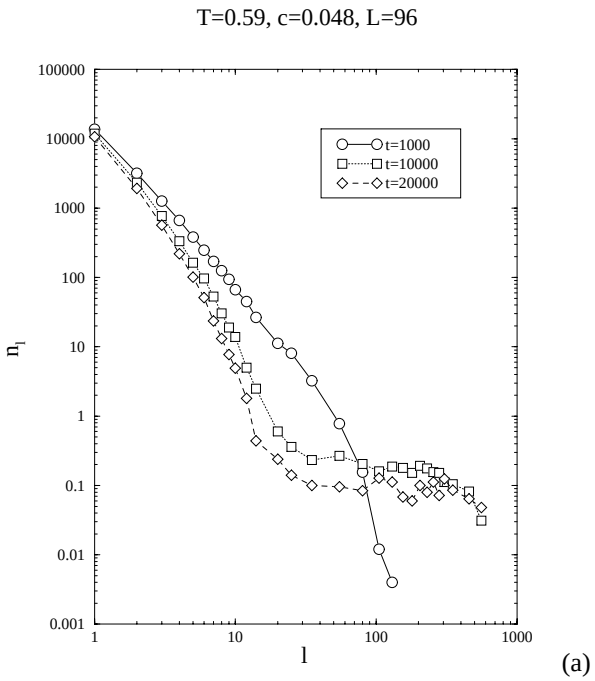

(a)

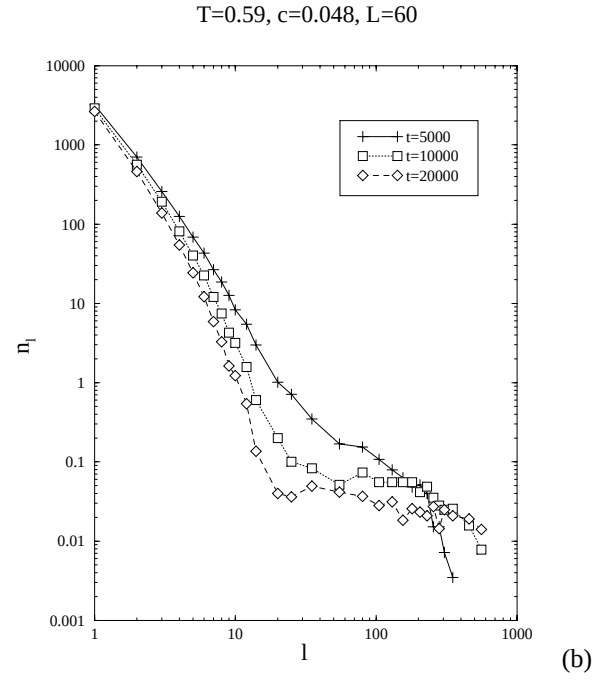

(b)

Figure 6: Time evolution of the cluster distribution following a quench

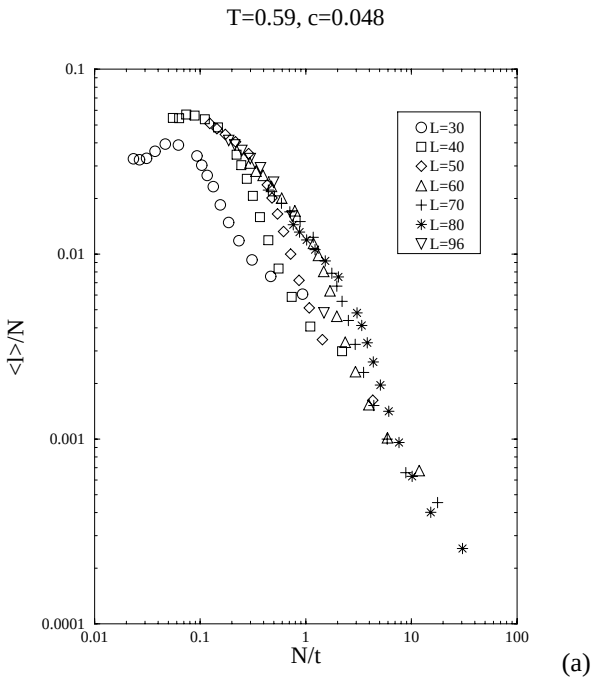

(a)

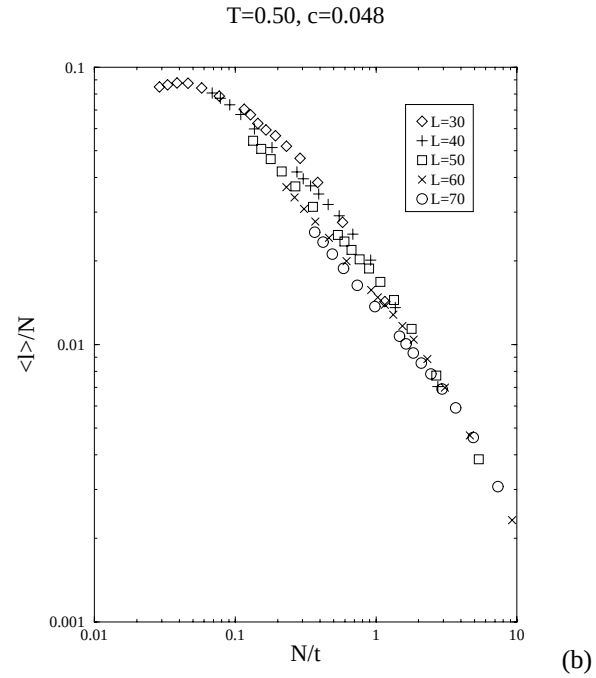

(b)

Figure 7: Finite size scaling plot of the average droplet size. Shown is the mean droplet volume $< l >$ rescaled by the volume and plotted as a function of the scaled time.

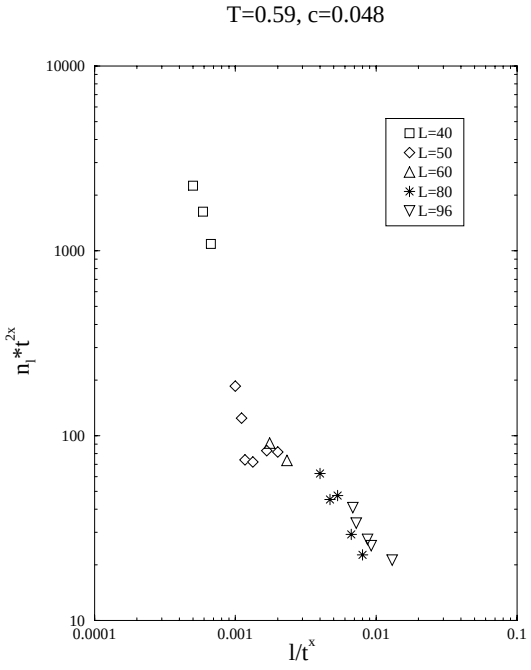

Figure 8: Scaling of the time evolution of the droplet concentration n_{l^*}